

Coronal Magnetic Field Measurements – Optical / IR

S. Tomczyk

High Altitude Observatory

National Center for Atmospheric Research



NCAR

High Altitude Observatory (HAO) – National Center for Atmospheric Research (NCAR)

The National Center for Atmospheric Research is operated by the University Corporation for Atmospheric Research under sponsorship of the National Science Foundation. An Equal Opportunity/Affirmative Action Employer.

30 Aug 2005

Motivation

“The most striking aspect of the subject of magnetic fields in the corona is the frequency and variety of situations for which they are postulated, compared to the scarcity of any definite information concerning them.”

from Donald E. Billings, *A Guide to the Solar Corona*, 1966.

Coronal Magnetic Field Measurement Techniques

Gyroresonant Emission: Radio Observations of Strong Field
Regions (>250 G) (*Kundu, Schmahl, Gerassimenko 1980*)

Hanle Effect: O VI 103.2 nm (*Sahal-Bréchet et al. 1986*)

Faraday Rotation: Radio Observations (*eg Hollweg et al. 1982*)

Longitudinal Zeeman Effect: (V, I) Coronal Emission Lines
(*Harvey 1968; Lin, Penn and Tomczyk 2000*)

Resonance Scattering: (Q, U, I) Coronal Emission Lines
(*KELP Instrument: Querfeld and Smartt 1984*)

Few Measurements Exist

Methodology

Line-of-Sight Field Strength derived from Longitudinal Zeeman effect in Stokes V profile. (Extremely difficult)

Plane-of-Sky Direction derived from Resonance Scattering effect in Stokes Q and U profiles

Line-of-Sight Velocity derived from Doppler effect in Stokes I

Plasma Density derived from Line Ratio in Stokes I

With I, Q, U, V , **vector magnetometry** is possible if information is available about the plasma

Challenges

- Low Coronal Photon Flux: for 1074.7, 20 cm aperture, 20 millionths Corresponds to 10^5 photons s^{-1} arcsec $^{-2}$
- Weak Fields ~ 10 G, Q , $U/I \sim 10^{-1}$, $V/I \sim 10^{-3} - 10^{-4}$
- Large Temporally Varying Background for Ground-Based Observations
- Need Large Aperture Telescope and Simultaneous Measurement of Quantities

Methodology

$$I \propto [1 + a\sigma (\cos^2 \Theta - \frac{1}{3})] \varphi(\omega - \omega_0)$$

$$Q \propto a\sigma \sin^2 \Theta \cos 2\Phi \varphi(\omega - \omega_0)$$

$$U \propto a\sigma \sin^2 \Theta \sin 2\Phi \varphi(\omega - \omega_0)$$

$$V \propto (\bar{g} + b\sigma) B \cos \Theta \varphi'(\omega - \omega_0)$$

$a, b \equiv$ constants depending on the spectral line
(for Fe XIII 1074.7 nm, $a = 1$, $b = 1.06$)

$\sigma \equiv$ *atomic alignment*, depending on scattering **geometry**
and **density** (for 1074.7 nm, $\sigma < .707$)

$\bar{g} \equiv$ *effective Landé factor* (for 1074.7 nm, $\bar{g} = 1.5$)

$\Theta \equiv$ inclination, $\Phi \equiv$ azimuth, $\varphi \equiv$ line profile (gaussian)

Methodology

If $\sigma \ll 1$ the **magnetograph formula** is obtained:

$$V \approx \bar{g} B \cos \Theta_B \frac{dI}{d\omega}$$

whereas from I , Q , and U , we get:

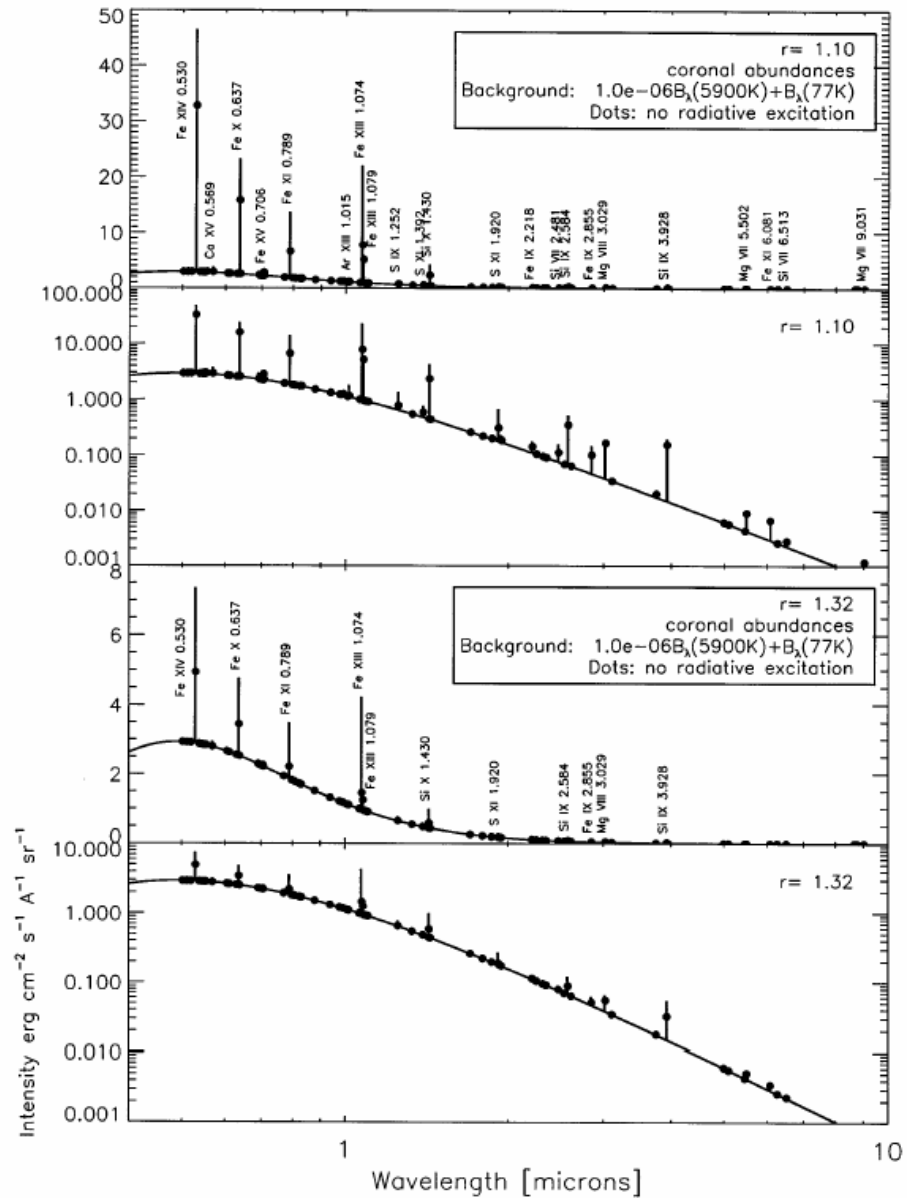
$$U/Q = \tan 2\Phi_B$$

valid for all $\sigma \neq 0$

$$P/I \equiv \frac{\sqrt{Q^2 + U^2}}{I} \approx |a\sigma| \sin^2 \Theta_B$$

Note: $\sigma \approx 0$ at the Van Vleck angle, Q,U subject to 90 degree ambiguity

Available Emission Lines



Judge, ApJ, 500, 1099, 1998.

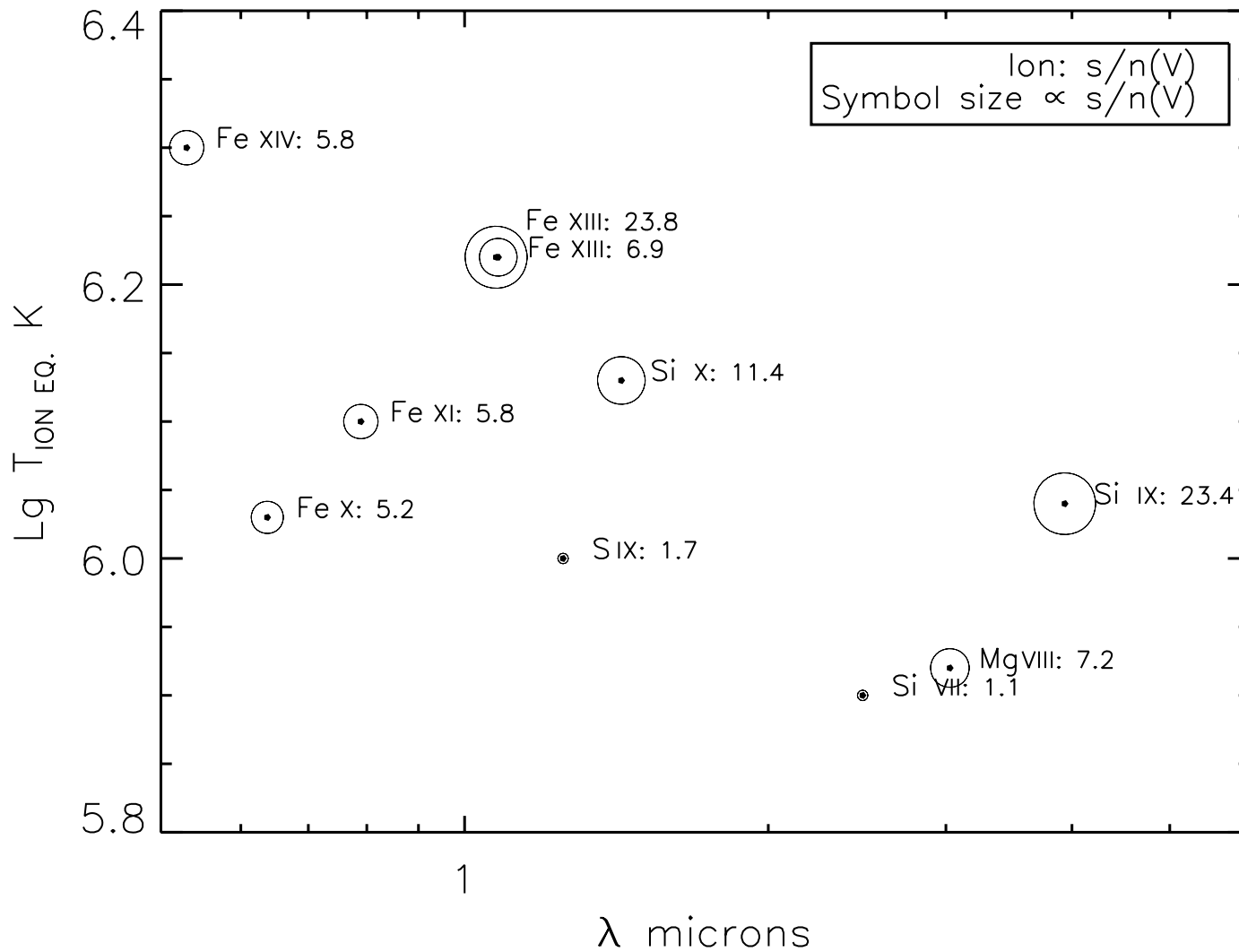


Stokes V Expected Precision

Table 8: Figures of Merit (Mauna Loa $D = 40$ cm at $1.1R_{\odot}$)

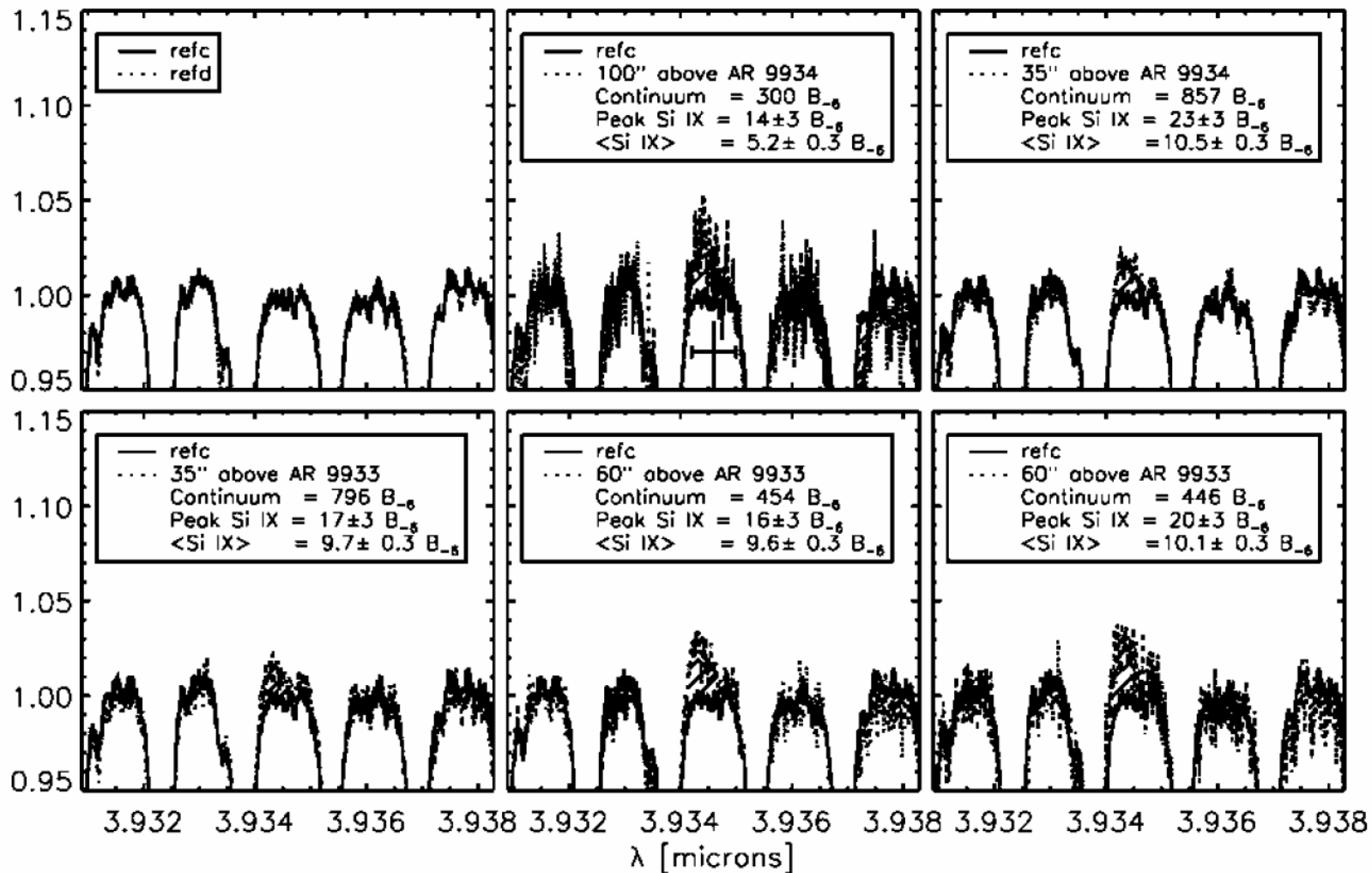
Ion	λ μm	Log I $\text{erg cm}^{-2} \text{s}^{-1} \text{sr}^{-1}$	Figure of merit (max s/n (V))	Max V/I	Log T_e
Fe XIII	1.0746	1.35	23.8	5.6-4	6.22
Si IX	3.9346	-0.17	23.4	1.5-3	6.04
Si X	1.4300	0.73	11.4	4.5-4	6.13
Mg VIII	3.027	-0.36	7.2	5.6-4	5.92
Fe XIII	1.0797	0.72	6.9	2.3-4	6.22
Fe XIV	0.5303	1.36	5.8	1.5-4	6.30
Fe XI	0.7891	0.96	5.8	1.8-4	6.10
Fe X	0.6374	1.12	5.2	1.5-4	6.03
S IX	1.252	-0.07	1.7	7.2-5	6.0
Si VII	2.481	-0.71	1.1	7.0-5	5.8

Note: The values of the “Figures of Merit” are simply maxima in the signal-to-noise ratios in Stokes V: therefore exceed the “typical” signal-to-noise ratios estimated in Section 3.2 above.



Judge, ApJ, 500, 1099, 1998.





Judge et al., ApJ, 576, L157, 2002.

Early Measurements

Linear Polarization Measurements of coronal Green line (530.3 nm) and FeXIII 1074.7 nm lines:

1960s: Charvin, Eddy, Hyder, Perche and others

1970s: Querfeld, Arnaud and others

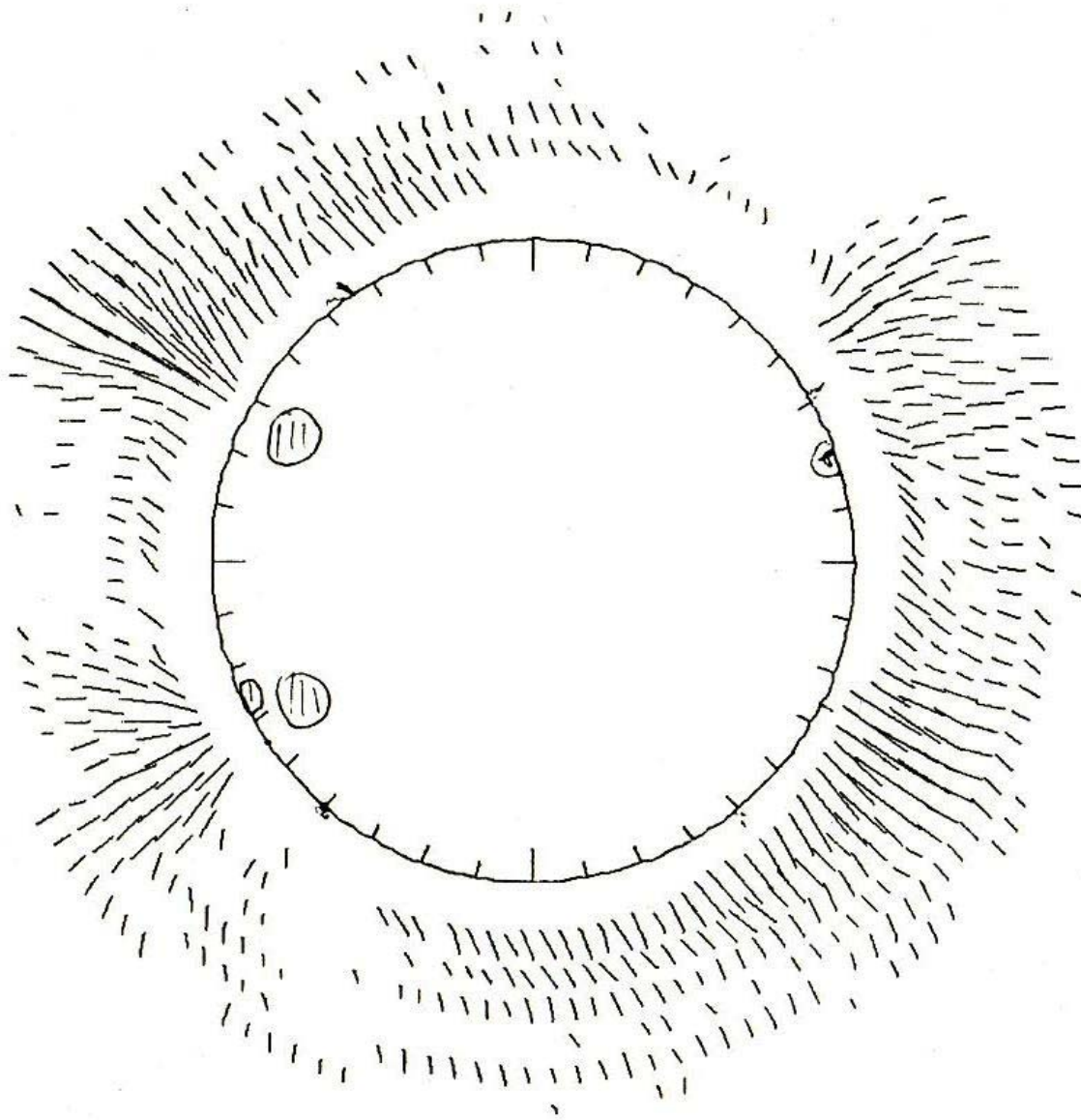
Other scattered eclipse measurements

Circular Polarization Measurements:

Green Line, Harvey (1969)

KELP - 1074.7 nm
14 Oct 1977

1 arcmin sampling
4 hours
vector lengths \sim pI



Arnaud, private communication.

Table 5-13

Measurements of coronal magnetic fields

Date (1967)	Time (UT)	PA ($^{\circ}$)	Aperture (arc-sec)	$B_{ }$ (gauss)	Nearby $B_{ }$ (gauss)
VII-3	1646-1716	73	30 x 60	13_{-20}^{+}	+
VII-19	1539-1644	119	30 x 60	-6_{-4}^{+}	-
VIII-11	1527-1607	58	30 x 60	-2_{-8}^{+}	-
VIII-12	1543-1603	113	30 x 60	-1_{-5}^{+}	-
IX-2	1551-1618	294	30 x 60	0_{-7}^{+}	$-3.6_{-0.3}^{+}$
X-12	1605-1633	304	14 x 356	$-1.5_{-0.5}^{+}$	$-4.0_{-0.7}^{+}$
(1968)					
I-21	1713-1815	110	15 x 330	$-2.0_{-0.7}^{+}$	-

Harvey, PhD thesis, 1969.

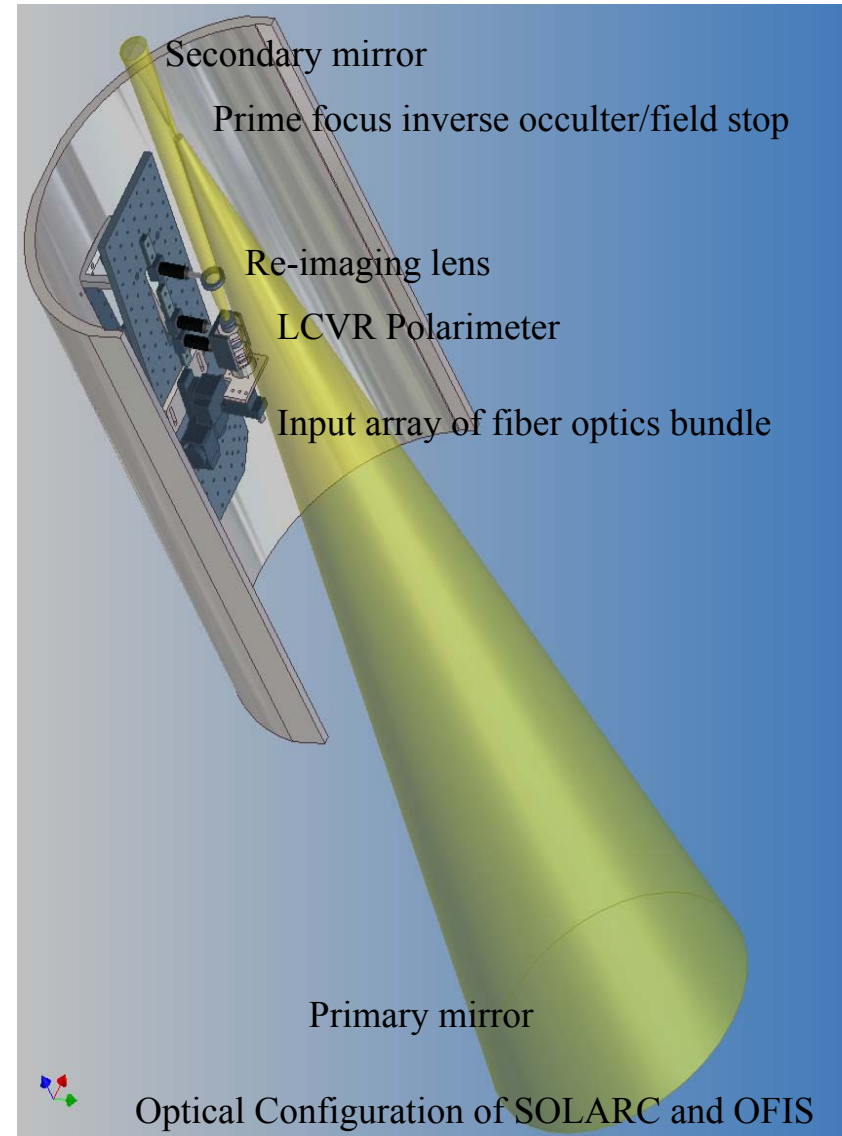


SOLARC: Off-Axis Mirror Coronagraph

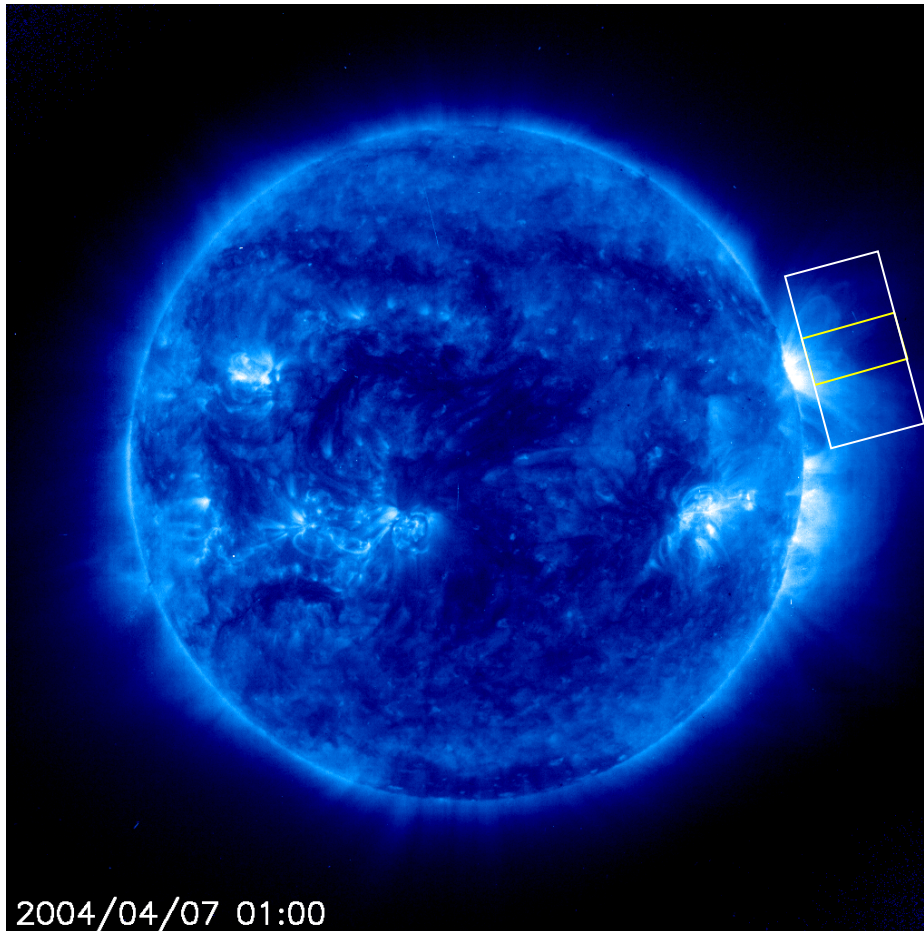
PI—Jeff Kuhn (IfA)

- 50 cm aperture off-axis gregorian telescope
- No secondary mirror and spider structure in the optical path for coronagraphic performance

SOLARC and its dome on the summit of Haleakala, Maui.



2004/04/06 Observation



Fe X 171Å image of the solar corona at approximately the time of SOLARC/OFIS observation from EIT 195 Å.

Full Stokes vector observations were obtained on April 6, 2004 on active region NOAA 0581 during its west limb transit.

Corona activity is low compared with the 1999 observations!

Stokes *I*, *Q*, *U*, & *V* Observation:

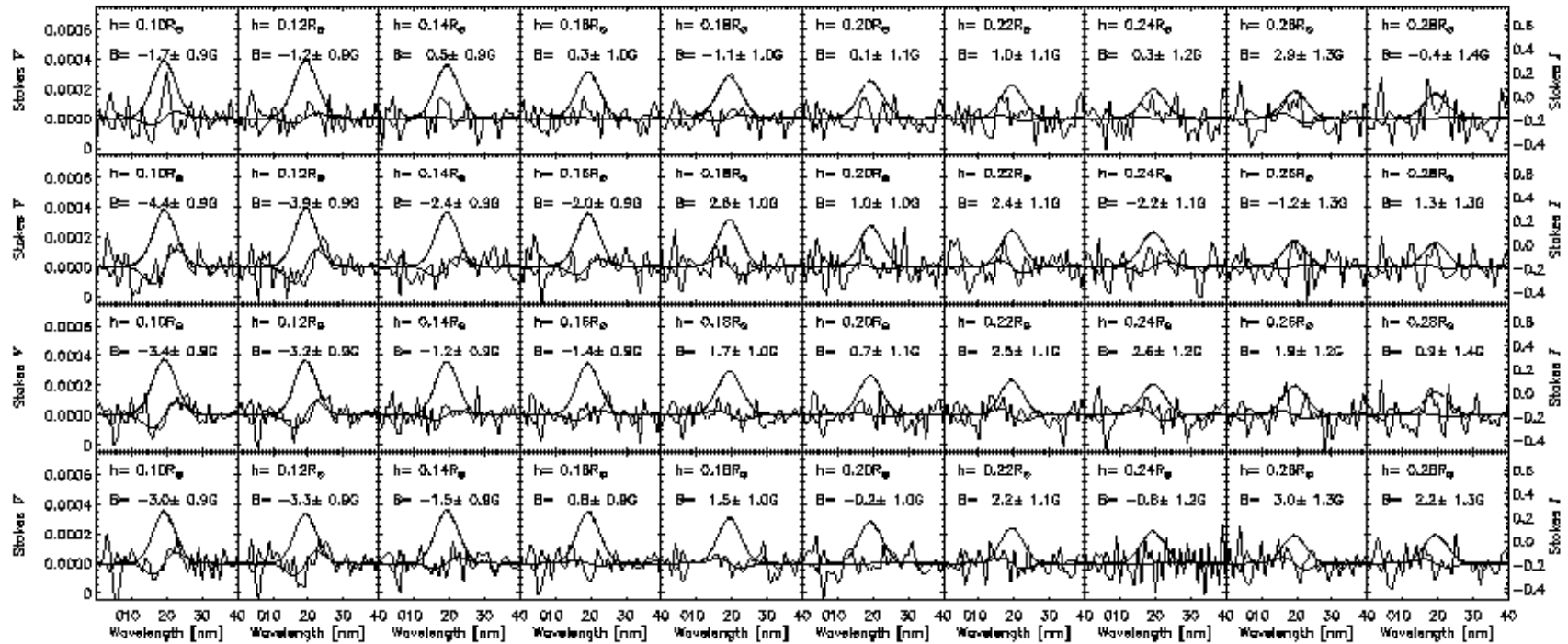
- 20arcsec/pixel resolution
- Telescope pointing @
Radius Vector $0.25 R_{\odot}$
Position Angle (Geocentric): 260° .
- ***70 minutes integration on V***
- ***15 minutes integration on Q & U***

Stokes *I*, *Q* & *U* Scan:

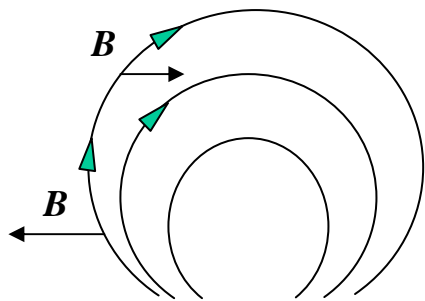
- $RV = 0.25 R_{\odot}$
- From PAG 250° to 270°
- Five 5° steps



Line-of-Sight Magnetic Fields



Samples of measured and fitted Stokes I and V spectra of the 10×4 ($200'' \times 80''$) pixel region closest to the solar limb. The errors of the magnetic fields are 1 sigma error. Geocentric north is up, and east is left.

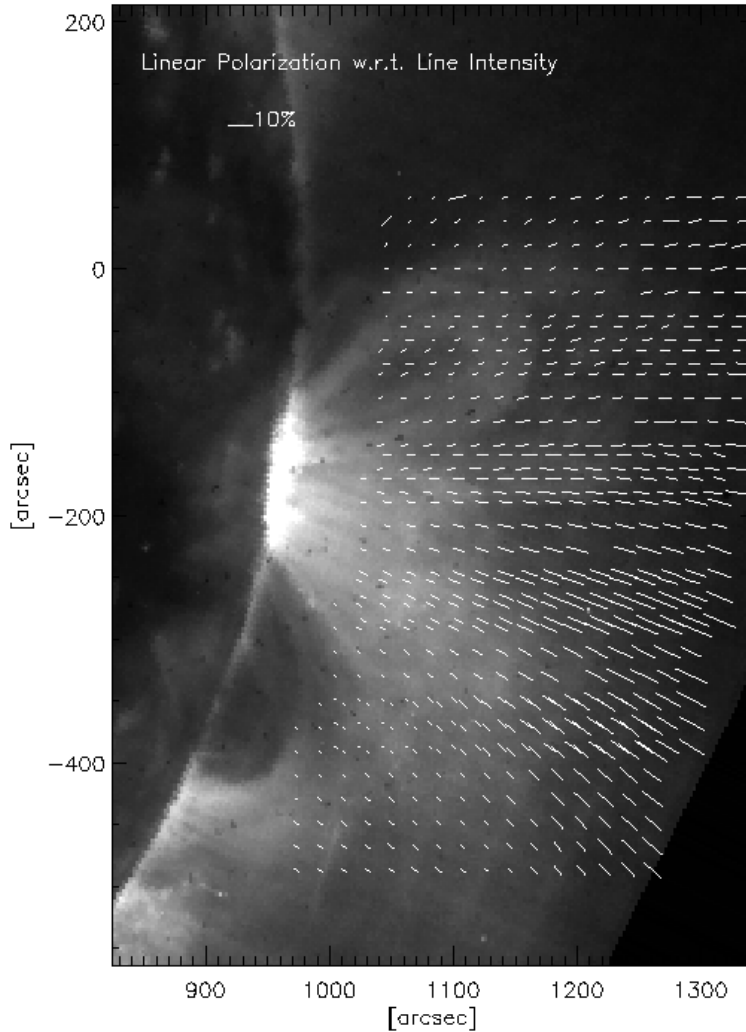


The longitudinal field reverses sign around $h=0.17 R_{\odot}$!

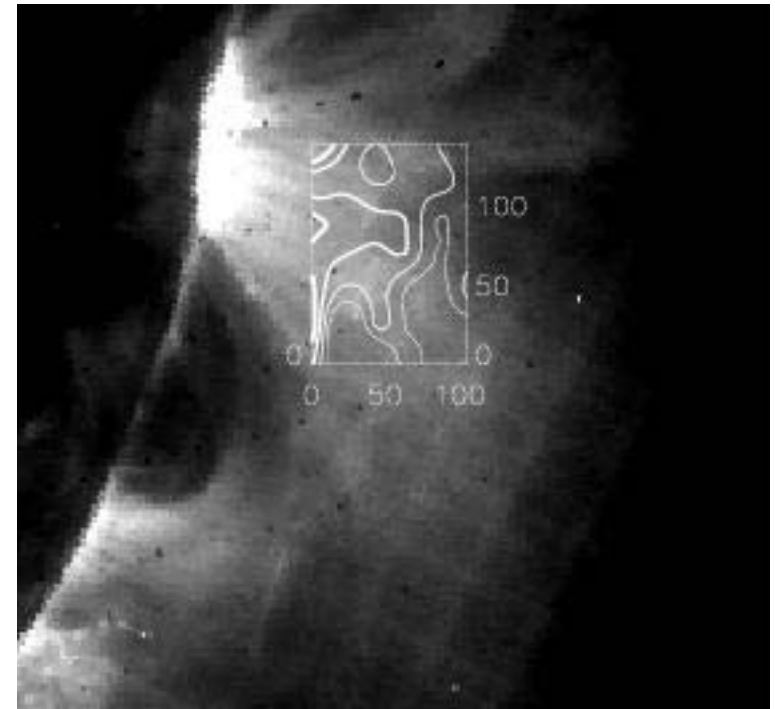


'Vector' Coronal Magnetogram

Transverse field orientation



Longitudinal Field Strength



Contour plot of the line-of-sight magnetogram over-plotted on the EIT FeXVI 284 A image. The contours are 5G, 3G, and 1G.

Our Approach

Based on: “*Coronal Magnetometry: A Feasibility Study*”, Judge, Casini, Tomczyk, Edwards, Francis, NCAR/TN 2001, we decided to:

Design and Construct a **Filter-Based Magnetograph**

Observe the **Corona** in the **Fe XIII** forbidden emission lines at 1074.7 and 1079.8 nm (1.6×10^6 K plasma)

Observe **Prominences** in **He I** 1083 nm



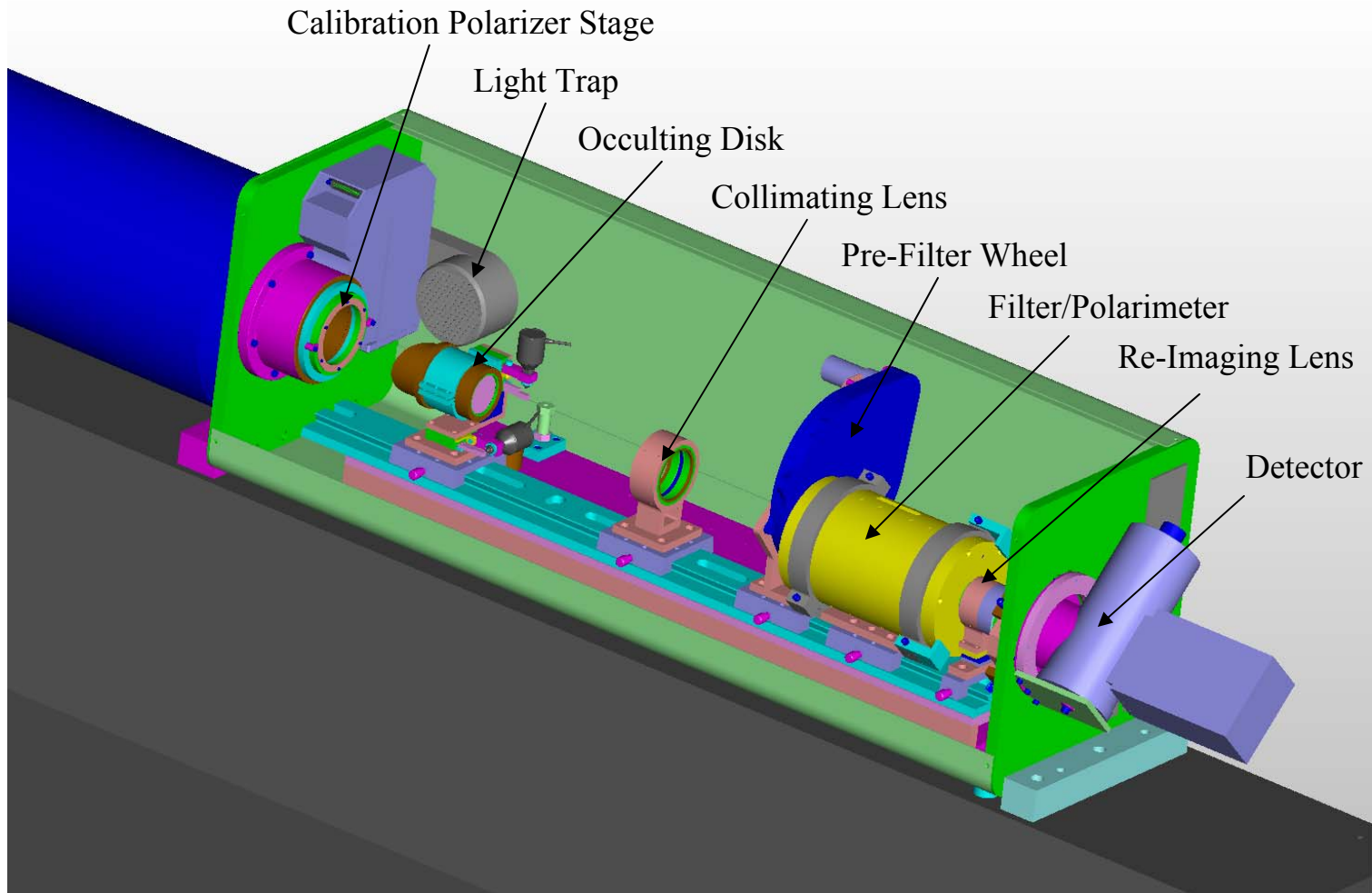
Coronal Magnetograph Design

- Filter Bandpass 0.14 nm FWHM for Optimal Magnetograph Based on Width of 1074.7 line
- Four Stage Calcite Wide-Field Lyot Filter with Liquid Crystal Tuning, Operating at 1074.7, 1079.8 and 1083.0 nm
- LC Polarization Analysis for Complete I, Q, U, V
- Polarizing Beamsplitter for Simultaneous Measurement of Image at 2 Wavelengths on Single Detector

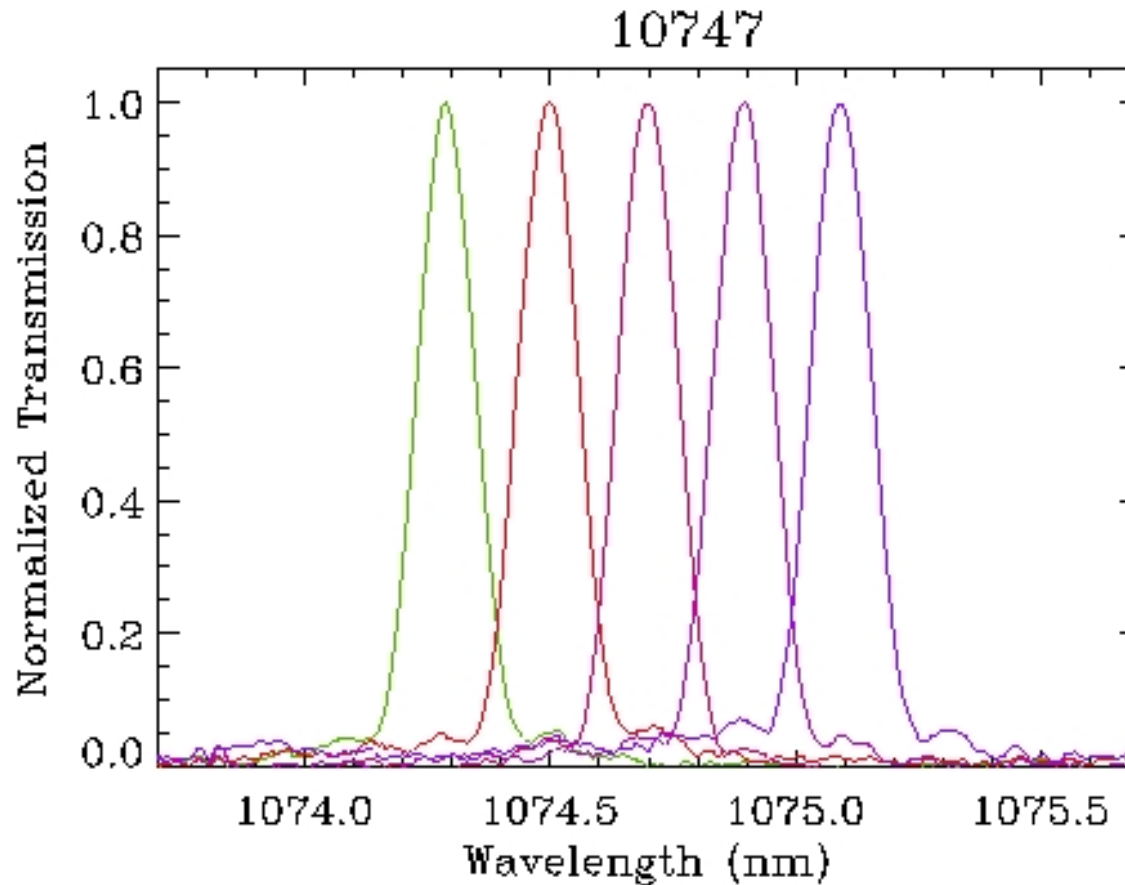
Coronal Multi-channel Polarimeter (CoMP)



Coronal Multi-channel Polarimeter (CoMP)



Measured Transmission Profiles



Filter has 30% maximum transmission to unpolarized light

Instrument Expected Performance

Assuming 20 millionths integrated emission in line (10 millionths through filter in line wing), 20 cm aperture, 4 arcsec pixels, and 7% system efficiency (atmosphere, telescope, filter, detector) gives $\sim 1 \times 10^5$ photons/pixel/s

Assuming photon noise and ideal sky conditions gives:

$$\sigma(\nu) = 148 \text{ m/s/pixel/sec}$$

$$\sigma(B_L) = 65 \text{ G/pixel/sec}$$

$$\sigma(\phi) = 0.94^\circ/\text{pixel/sec}$$

Instrument Implementation

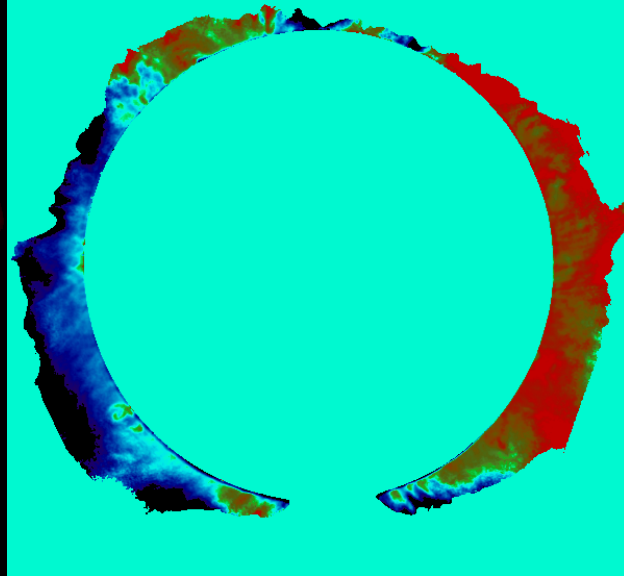


- Corona - Fe XIII 1074.4, 1079.8, Prominence - He I 1083.0
- Measure 2 Wavelengths Simultaneously
- 1024 x 1024 HgCdTe Detector, $\pm 1.4 R_{\text{sun}}$ Field-of-View, 4.5 arcsec/pixel
- Sac Peak 20 cm “One Shot” Coronagraph (R.N. Smartt, et al., 1981)
- Initial Deployment Jan 2004
First 1083.0 Data, March 2004
First 1074.7 Data, May 2004

FeXIII 1074.7 Intensity 4/21/05



FeXIII 1074.7 Line-of-Sight Velocity 4/21/05



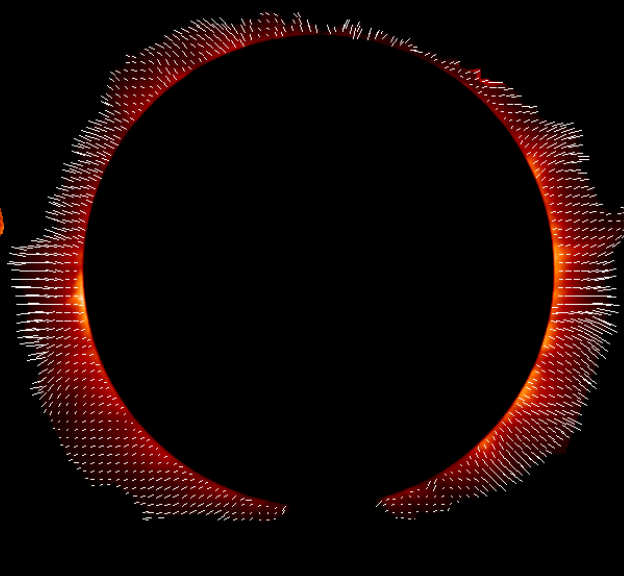
FeXIII 1074.7 Linear Polarization 4/21/05



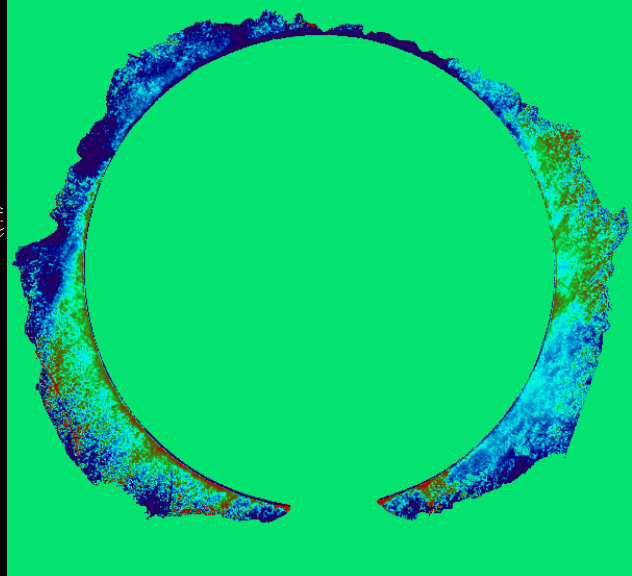
FeXIII 1074.7 Line Width 4/21/05



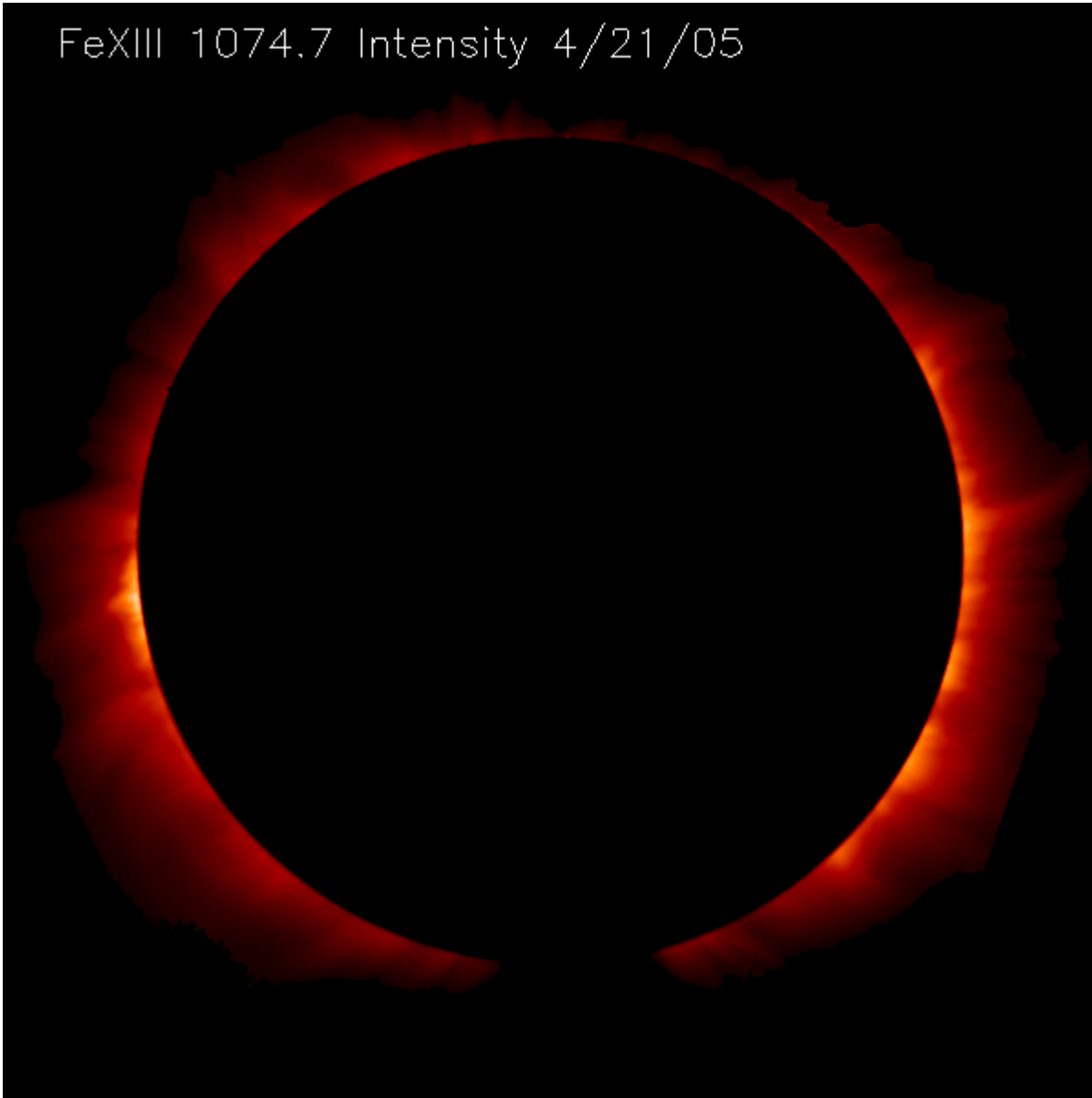
FeXIII 1074.7 Azimuth of B 4/21/05



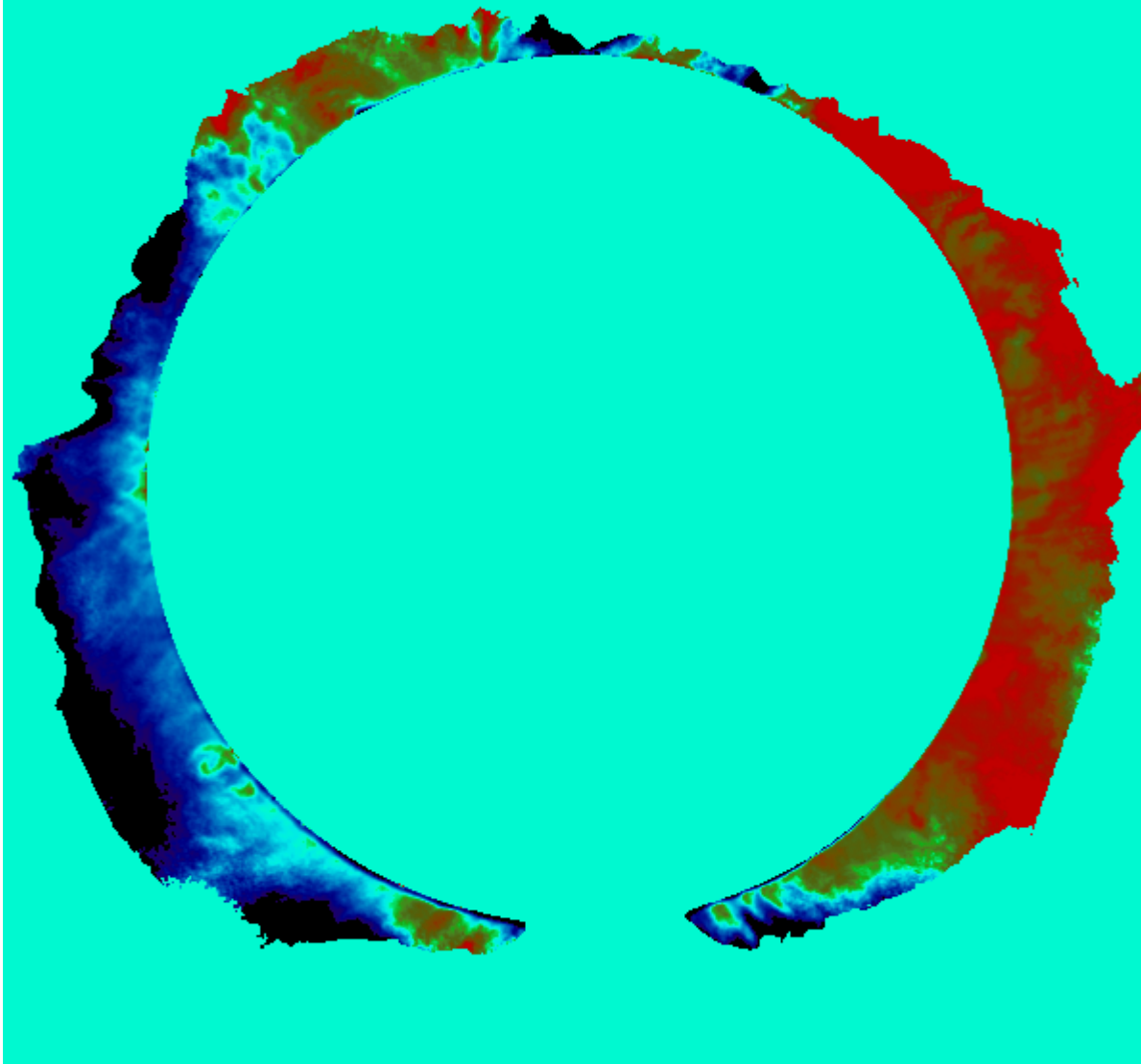
FeXIII 1074.7 Longitudinal B 4/21/05



FeXIII 1074.7 Intensity 4/21/05



FeXIII 1074.7 Line-of-Sight Velocity 4/21/05



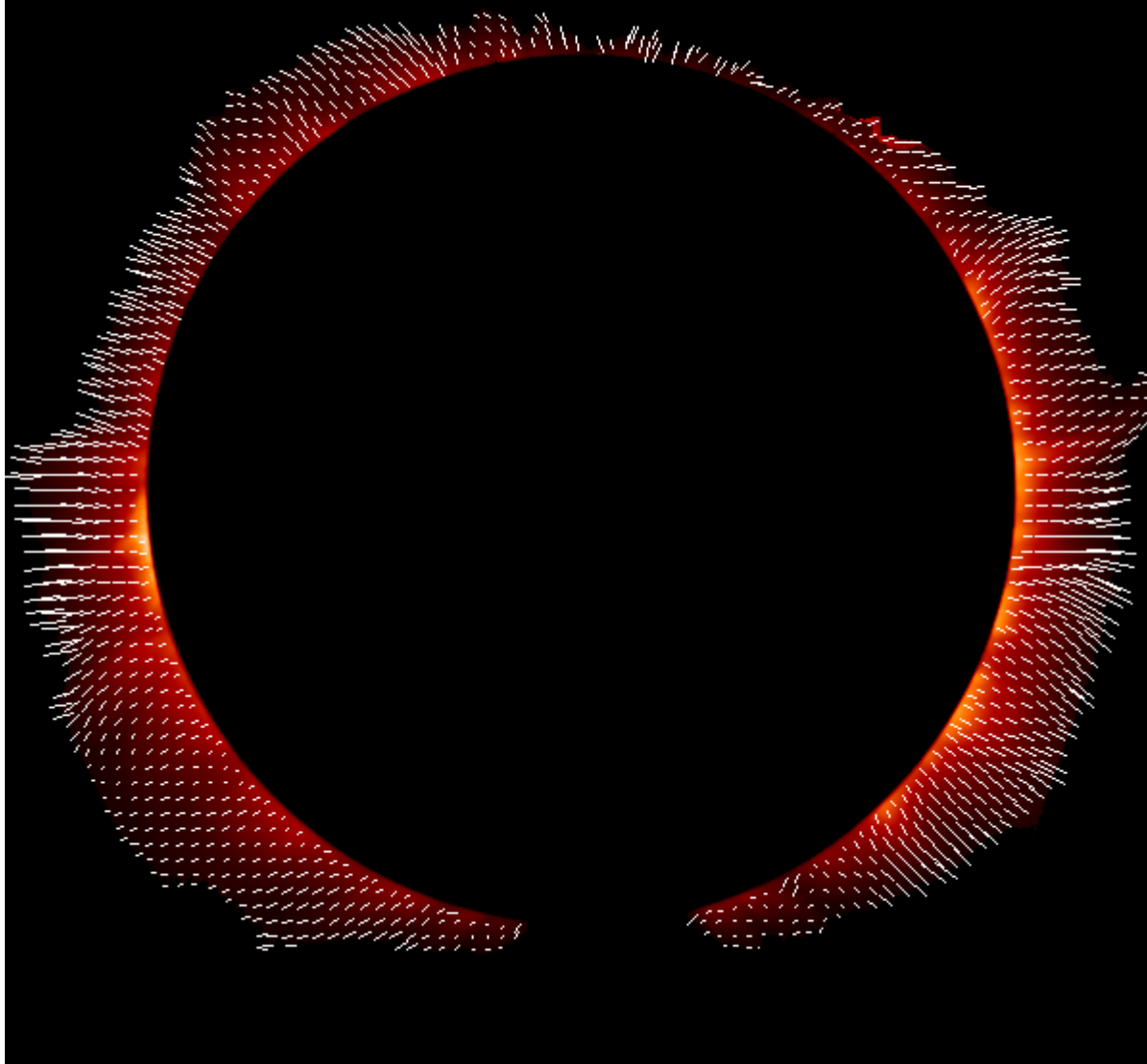
FeXIII 1074.7 Linear Polarization 4/21/05



FeXIII 1074.7 Line Width 4/21/05

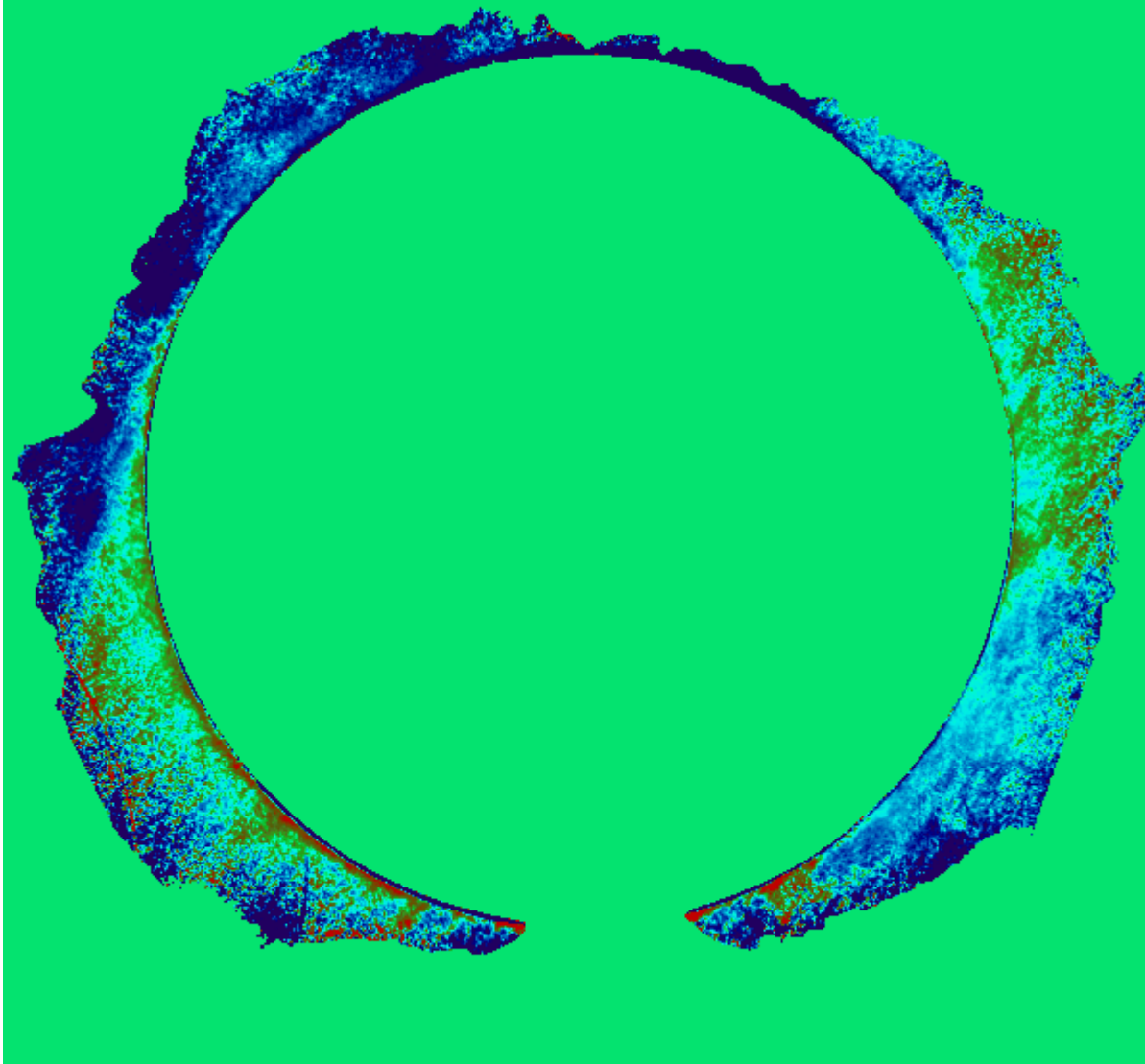


FeXIII 1074.7 Azimuth of B 4/21/05



8x8 pixels

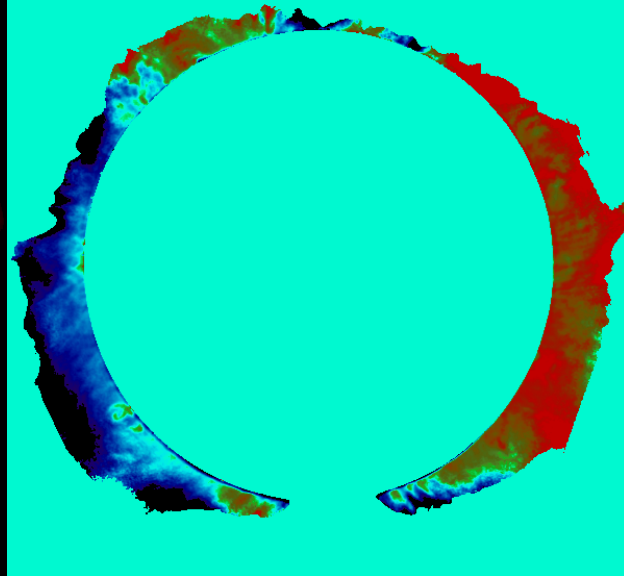
FeXIII 1074.7 Longitudinal B 4/21/05



FeXIII 1074.7 Intensity 4/21/05



FeXIII 1074.7 Line-of-Sight Velocity 4/21/05



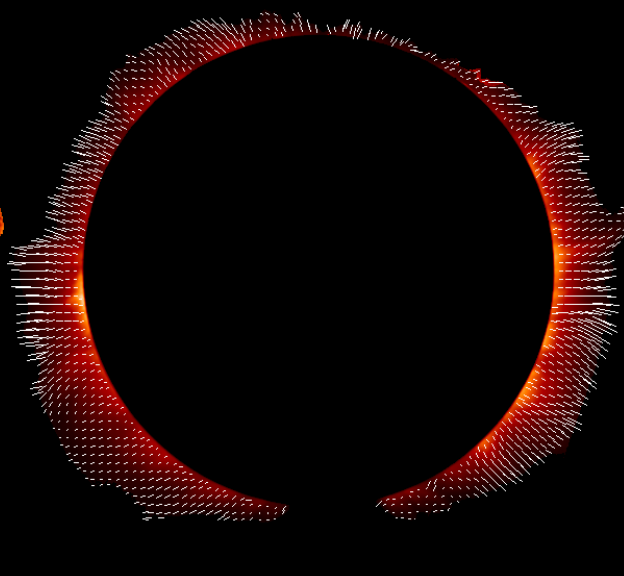
FeXIII 1074.7 Linear Polarization 4/21/05



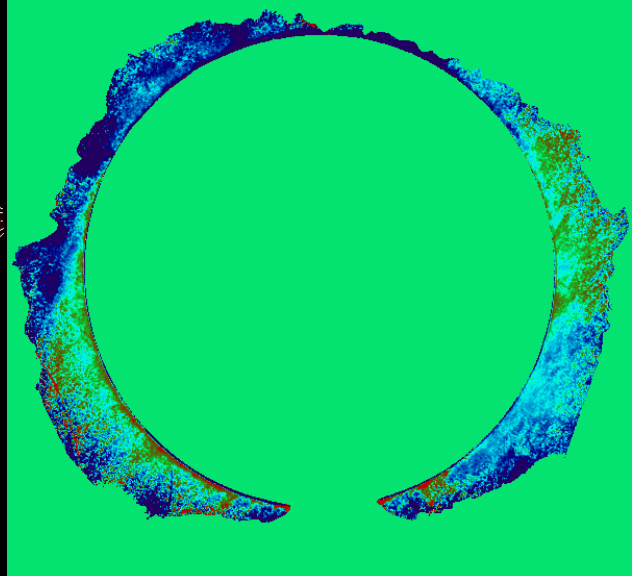
FeXIII 1074.7 Line Width 4/21/05

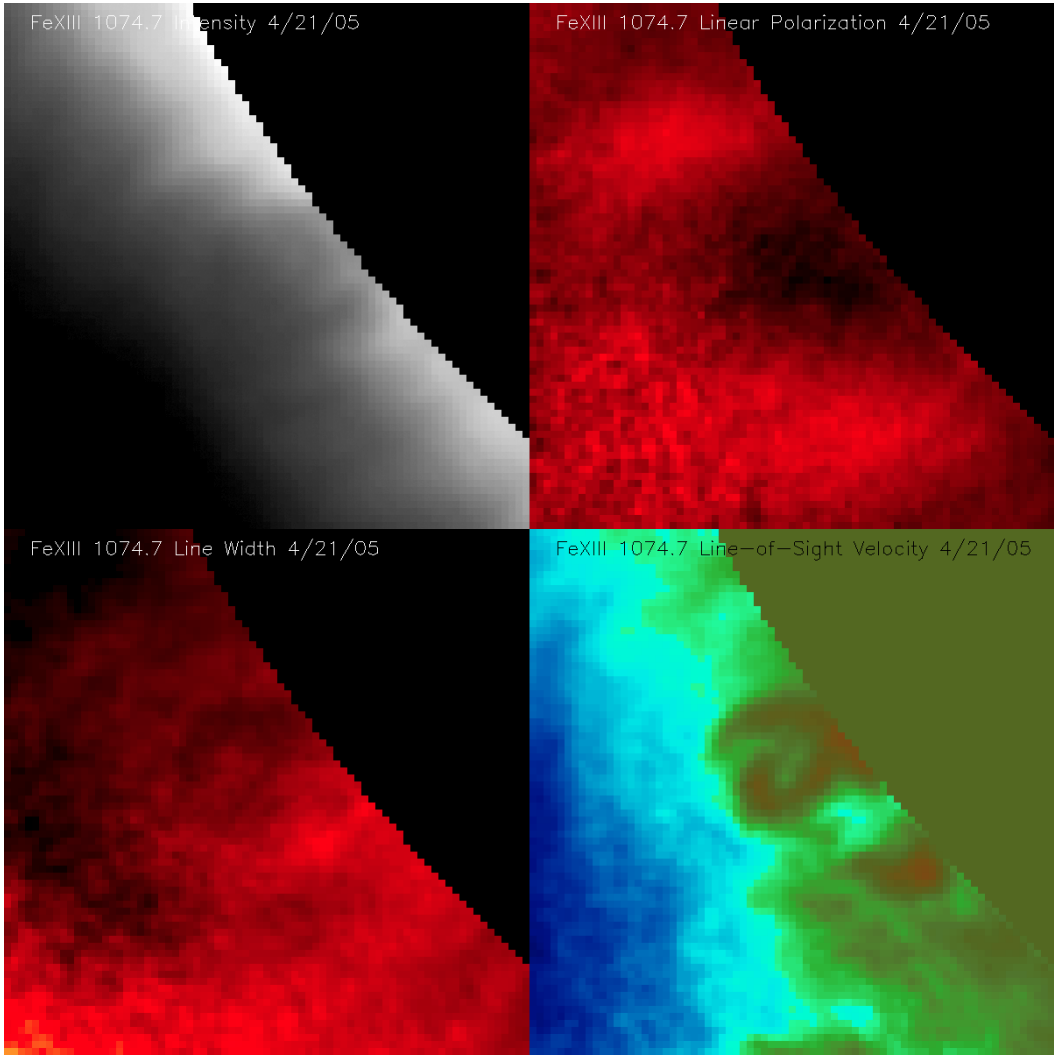


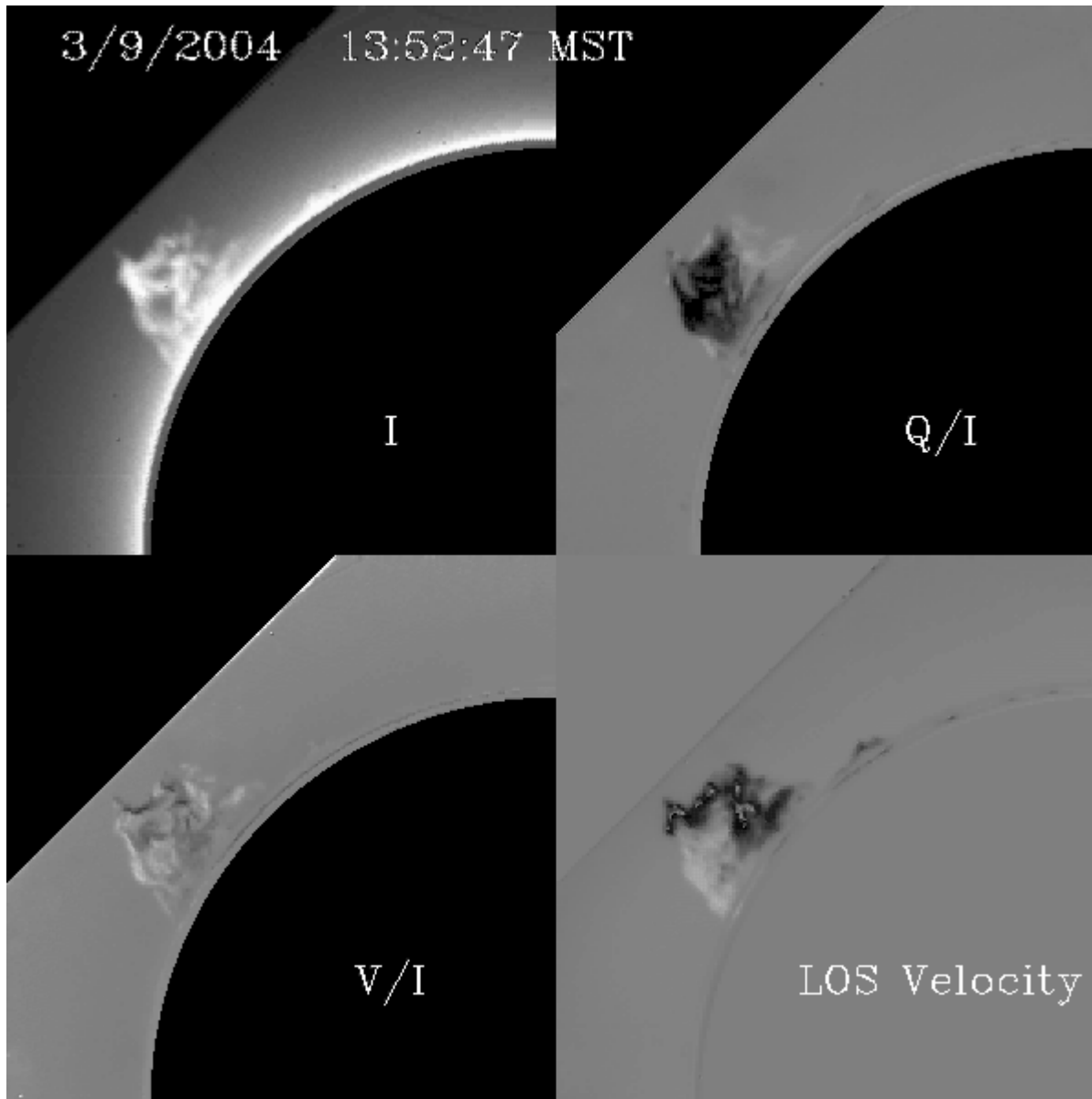
FeXIII 1074.7 Azimuth of B 4/21/05



FeXIII 1074.7 Longitudinal B 4/21/05

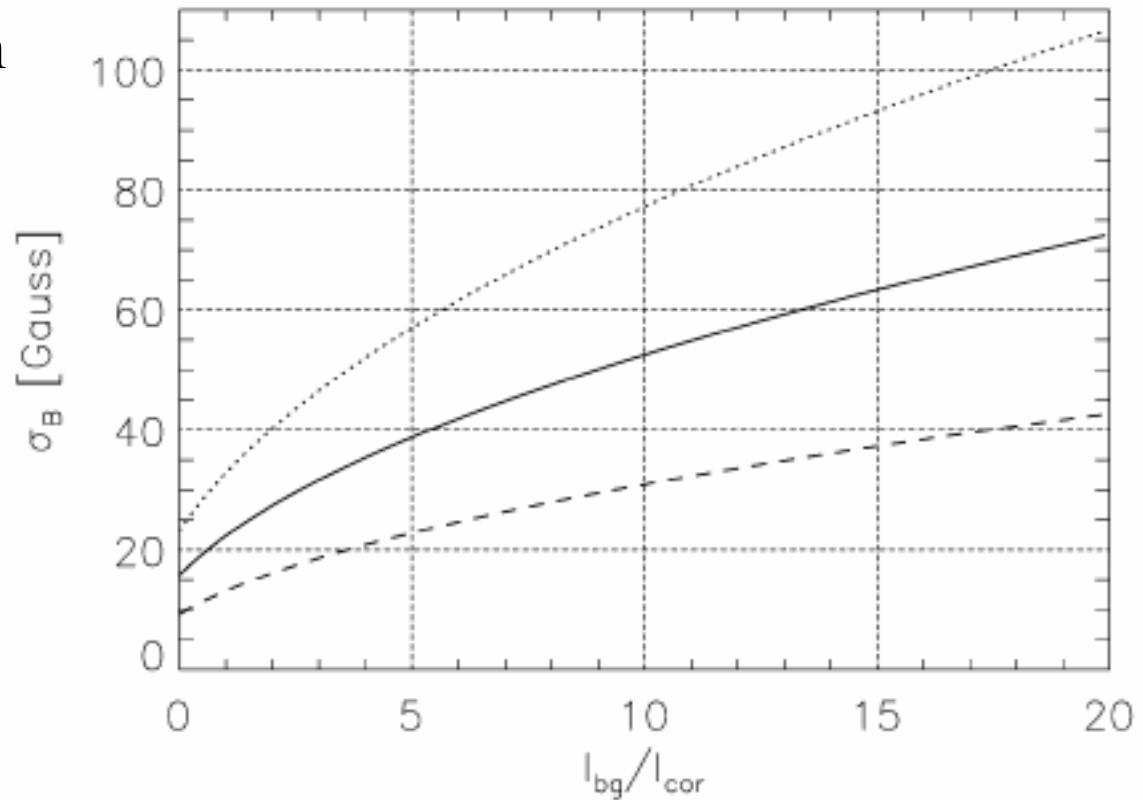






ATST Expected Performance

4 meter aperture
1 arcsec pixels
1 second integration
40 millionths



Penn et al., Sol Phys, 222, 61, 2004.



Large Synoptic Coronagraph

For 20 millionths 1074.7, 4 Beam system, 1 m aperture
and 2 arcsec pixels

$$\sigma(v) = 47 \text{ m/s/pixel/sec}$$

$$\sigma(B_L) = 21 \text{ G/pixel/sec}$$

$$\sigma(\phi) = 0.30^\circ/\text{pixel/sec}$$

0.86 G in 10 minutes

0.35 G in 1 hour